ELSEVIER

Journal of Organometallic Chemistry 578 (1999) 85–90

Journal of Organometallic Chemistry

Organometallic C_{70} chemistry. Preparation and crystallographic studies of $(\eta^2\text{-}C_{70})Pd(PPh_3)_2 \cdot CH_2Cl_2$ and $(C_{70}) \cdot 2\{(\eta^5\text{-}C_5H_5)_2Fe\}$

Marilyn M. Olmstead, Leijun Hao, Alan L. Balch *

Department of Chemistry, University of California, Davis, CA 95616, USA

Received 8 July 1998

Abstract

Treatment of a solution of C_{70} with solutions of $Pd(PPh_3)_4$ or ferrocene result in the formation of either black–brown $(\eta^2\text{-}C_{70})Pd(PPh_3)_2 \cdot CH_2Cl_2$ or metallic-black $C_{70} \cdot 2\{(\eta^5\text{-}C_5H_5)_2Fe\}$, respectively. Crystallographic examination of the palladium complex reveals that the metal is coordinated to the a–b bond (a highly pyramidalized 6:6 ring junction) at the pole of the fullerene. The variable temperature ^{31}P-NMR spectrum of the complex reveals the coalescence of the two doublets of the adduct at 80°C. This merging of the resonances results from a dynamic process that may involve rotation of the olefinic fullerene bond about the plane of the PdP_2 unit or phosphine dissociation. X-ray crystallography of the ferrocene-containing compound, $C_{70} \cdot 2\{(\eta^5\text{-}C_5H_5)_2Fe\}$, reveals that it involves co-crystallization of two ordered ferrocene molecules with an ordered C_{70} molecule with no unusual interaction between these entities. The structure is similar in many aspects to that of $C_{60} \cdot 2\{(\eta^5\text{-}C_5H_5)_2Fe\}$.

Keywords: Fullerene; Ferrocene; Palladium; C_{70}

1. Introduction

Considerable effort has been made in the investigation of the reactions of transition metal complexes with C_{60} [1–3]. The major reactions encountered include (1) coordination, generally in an η^2-fashion to the olefinic 6:6 ring junctions of the fullerene, (2) reduction of the fullerene to form fulleride salts, (3) addition of a ligating group on the metal complex to the fullerene so that the metal is attached to the fullerene through some type of covalent bridge, and (4) formation of a solid in which a metal complex and the fullerene are co-crystallized [1]. Considerably less attention has been give to the behavior of the higher, but less abundant, fullerenes with metal complexes. There are a few reports on the behavior of C_{70} with transition metal complexes [4–9] but only one in which C_{76} is utilized [10]. One paper involving osmylation of C_{78} has also appeared [11], and two papers describe interactions of C_{84} with transition metal complexes [11,12]. Here we report on the preparation of two new compounds that result from the interaction of C_{70} with transition metal complexes. The observed reactions reported here include one case of η^2-coordination and one case of co-crystallization.

As seen in Fig. 1, the structure of C_{70} is more complex than that of C_{60}; since the former contains five distinct types of carbon atoms while the later contains only one type of carbon atom. There are two types of C–C bonds in C_{60}, those at 6:6 ring junctions and those at 6:5 ring junctions. C_{70} also has 6:6 and 6:5 ring junctions, but there are four distinct 6:6 ring junctions (a–b, c–c, d–e and e–e) and four 6:5 ring junctions (a–a, b–c, c–d and d–d) in this fullerene. Previous work has shown that metal complexes that coordinate to C_{70} in an η^2-fashion selectively add to the a–b bonds at the ends of the fullerene [4,5,7]. These bonds involve the most pyramidalized carbon atoms within the fullerene [13], and these atoms undergo further pyramidalization upon coordination.

* Corresponding author.

0022-328X/99/$ - see front matter
PII: S0022-328X(98)01108-5

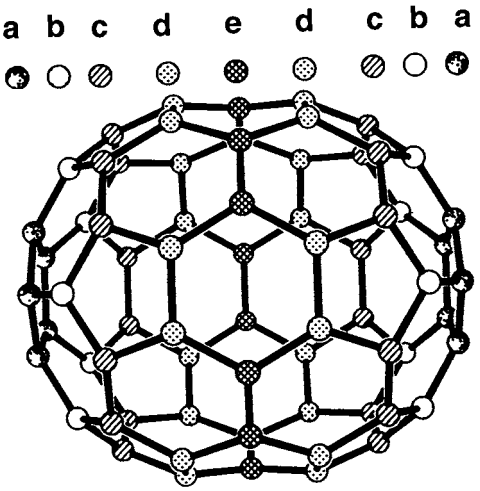

Fig. 1. An drawing of an idealized C_{70} molecule that shows the five types of carbon atoms (a–e) and the eight types of C–C bonds.

2. Results

2.1. Formation and solution properties of $(\eta^2\text{-}C_{70})Pd(PPh_3)_2$

Brown–black $(\eta^2\text{-}C_{70})Pd(PPh_3)_2$ was readily formed in high yield by mixing equimolar amounts of $Pd(PPh_3)_4$ and C_{70} in benzene as shown in Eq. (1).

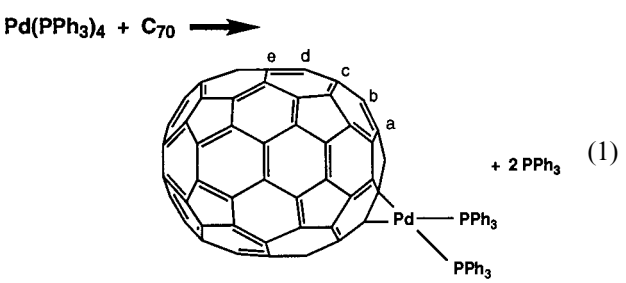

(1)

The reaction was monitored by ^{31}P-NMR spectroscopy and was complete almost immediately after mixing. After evaporation of the solvent, the product was dissolved in dichloromethane, filtered and crystallized through the addition of diethyl ether. The product, $(\eta^2\text{-}C_{70})Pd(PPh_3)_2$, is moderately stable in air in the solid state but decomposes slowly in solution when exposed to air. The ^{31}P-NMR spectrum of the complex in toluene-d_8 consisted of a pair of doublets at 29.2 and 26.7 ppm at -80°C with $^2J(P^a, P^b)$ of 8 Hz. Thus, the two phosphorus atoms of the complex are inequivalent, which is consistent with coordination of the palladium to the 6:6 ring junctions that involve either the a–b or c–d bonds (see Fig. 1) within the fullerene. Additionally, the ^{31}P-NMR spectrum of the reaction product always also showed the presence of two resonances at $\delta = 28.8$ and 26.4, respectively, at -80°C. These resonances had ca. 10% of the intensity of the major doublet, and are believed to result from the presence of a second isomer of $(\eta^2\text{-}C_{70})Pd(PPh_3)_2$. Attempts to separate and isolate the isomer responsible for these low intensity resonances by selective crystallization have not been successful.

The ^{31}P-NMR spectrum of $(\eta^2\text{-}C_{70})Pd(PPh_3)_2$ is sensitive to temperature. Warming from -80 to 25°C produces a broadening of the resonances so that the doublet structure is no longer apparent, and further warming produces added broadening until the resonances coalesce into a broad singlet at 27.9 ppm at 80°C and then sharpen as the temperature is increased to 100°C. Upon cooling the changes described here are reversed. This behavior is attributed to a dynamic process in which the environments of the two phosphorus atoms of the complex are rendered equivalent. Simple rotation about the Pd–olefinic C–C bond of the fullerene accomplishes such an interchange. This process is shown diagramatically in Eq. (2). Alternatively, the phosphine ligands may undergo dissociation and reassociation.

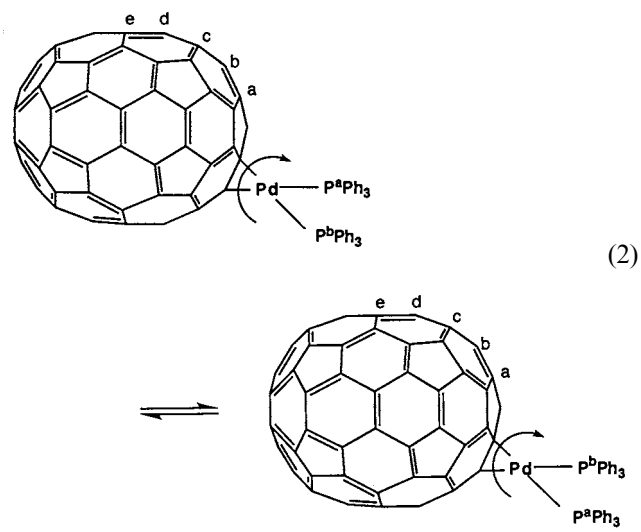

(2)

2.2. The crystal and molecular structure of $(\eta^2\text{-}C_{70})Pd(PPh_3)_2$

A view of the molecule, which has no crystallographically imposed symmetry, is shown in Fig. 2. Selected bond distance and angles are contained in Table 1. The complex consists of a $Pd(PPh_3)_2$ unit that is bonded through palladium in an η^2-fashion to one of the a–b bonds of the C_{70} molecule. Coordination of the C(1)–C(6) bond of the fullerene results in an elongation of that bond (bond length, 1.48(2) Å) relative to the expected length (1.39 Å) of such an a–b bond in C_{70}. The bond distances and angles reported here are all similar to those found for $(\eta^2\text{-}C_{60})Pd(PPh_3)_2$ [14]. The overall structure is also similar to that reported earlier from this laboratory for $(\eta^2\text{-}C_{70})Ir(CO)Cl(PPh_3)_2$ [4]. Not only is the metal bonded to the fullerene in the two

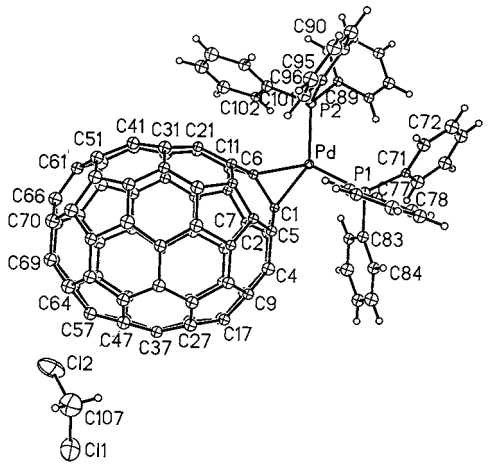

Fig. 2. A perspective view of $(\eta^2\text{-}C_{70})Pd(PPh_3)_2 \cdot CH_2Cl_2$. The distances from the dichloromethane molecule to the fullerene are: Cl(2)···C(47), 3.31 Å, Cl(2)···C(57), 3.50 Å; Cl(1)···C(31′), 3.41 Å, Cl(1)···C(40′), 3.41 Å.

complexes in the same η^2-fashion, but two of the phenyl rings of the triphenylphosphine ligands make face-to-face contact with the surface of the C_{70} portion of both the palladium and the iridium complex.

2.3. Formation and structure of $C_{70} \cdot 2\{(\eta^5\text{-}C_5H_5)_2Fe\}$

Gradual evaporation of a solution of C_{70} and ferrocene in carbon disulfide results in the deposition of large thin plates of $C_{70} \cdot 2\{(\eta^5\text{-}C_5H_5)_2Fe\}$ which are co-mingled with orange crystals of ferrocene itself. The plates of $C_{70} \cdot 2\{(\eta^5\text{-}C_5H_5)_2Fe\}$, which have a silvery sheen, were manually separated form the orange ferrocene crystals for examination by X-ray crystallography.

Views of the structure of $C_{70} \cdot 2\{(\eta^5\text{-}C_5H_5)_2Fe\}$ are shown in Figs. 3 and 4. The solid is comprised of individual molecules of the two components with no covalent bonding between these molecules. Despite the tendency of individual fullerene molecules to display disorder in the solid state, both the C_{70} and the ferrocene molecules are ordered within this solid. Dimensions within the ferrocene portion are normal; the average Fe–C distance is 2.04 Å. Average C–C distances within the C_{70} molecule are given in Table 2, where they are compared with related structure determinations of C_{70} in various forms. Fig. 3 shows the way in which two ferrocene molecules pack near the ends of the oblong C_{70} molecule so that the two pentagonal faces on the C_5 axis of the fullerene make van der Waals $\pi-\pi$ contact with ferrocene molecules. The distances between the carbon atoms of the fullerene and the ferrocene molecule fall in the range 3.3–3.4 Å, which is what is expected from contacts between aromatic molecules and the separation of planes in graphite (3.35 Å). Fig. 4 is a stereoscopic view of the molecular organization within the solid.

Table 1
Selected bond distances and angles for $(\eta^2\text{-}C_{70})Pd(PPh_3)_2 \cdot CH_2Cl_2$

Bond length (Å)			
Pd–C(1)	2.106(11)	Pd–C(6)	2.123(11)
Pd–P(1)	2.328(3)	Pd–P(2)	2.340(3)
C(1)–C(6)	1.48(2)		
Bond angles (°)			
C(1)–Pd–C(6)	41.1(4)	C(1)–Pd–P(1)	100.2(3)
C(1)–Pd–P(2)	143.6(3)	C(6)–Pd–P(1)	140.6(3)
C(6)–Pd–P(2)	102.5(3)	P(1)–Pd–P(2)	115.62(11)

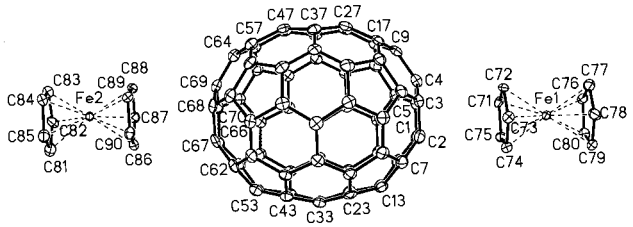

Fig. 3. A view of the structure of $C_{70} \cdot 2\{(\eta^5\text{-}C_5H_5)_2Fe\}$ showing the face-to-face interactions of the poles of the fullerene with adjacent ferrocene molecules.

Ferrocene forms a similar crystalline compound with C_{60} [15]. Although $C_{70} \cdot 2\{(\eta^5\text{-}C_5H_5)_2Fe\}$ and $C_{60} \cdot 2\{(\eta^5\text{-}C_5H_5)_2Fe\}$ crystallize in different space groups, the two structures are similar. Fig. 5 shows the two structures from a perspective that demonstrates the similarities between them. In both solids there are face-to-face π contacts between the fullerene and the ferrocene molecules. Additionally, in both structures the ferrocene molecules have an eclipsed conformation of the two cyclopentadienyl rings. In crystalline ferrocene itself the two rings are eclipsed [16]. However, the barrier to rotation is low (ca. 5 kJ mol^{-1} or less) and in the gas phase the rings are eclipsed [17]. Consequently, either eclipsed or staggered configurations can be found for ferrocene-based compounds [18].

3. Discussion

Structural characterization of $(\eta^2\text{-}C_{70})Pd(PPh_3)_2$ confirms our earlier studies of addition patterns of metal complexes to C_{70} [4,5,7]. Addition of $Pt(PPh_3)_2$ units to C_{70} was shown to produce four compounds, $(\eta^2\text{-}C_{70})\{Pt(PPh_3)_2\}_n$ (with $n = 1$, 2, 3 and 4) [7]. Spectroscopic data suggested that the first and second platinum atoms are bound to the a–b bonds at opposite ends of the fullerene, while the third and fourth added to the c–c bonds. Crystallographic characterizations of $(\eta^2\text{-}C_{70})Pd(PPh_3)_2$ and $(\eta^2\text{-}C_{70})\{Pt(PPh_3)_2\}_4$ support this suggestion. The structure of $(\eta^2\text{-}C_{70})Pd(PPh_3)_2$ reveals coordination to the a–b bond at one end of the

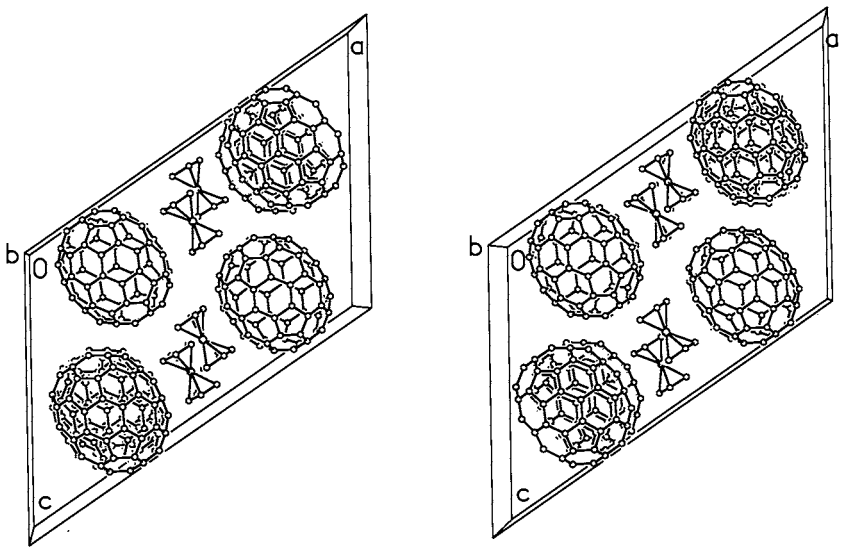

Fig. 4. A stereo view of the structure of $C_{70} \cdot 2\{(\eta^5\text{-}C_5H_5)_2Fe\}$.

fullerene, while the structure of $(\eta^2\text{-}C_{70})\{Pt(PPh_3)_2\}_4$ showed that the four platinum atoms were arranged in a C_{2v} symmetric fashion with coordination at two a–b and two c–c bonds [7].

In the absence of a coordinated group, which lowers the symmetry of the fullerene, molecules of C_{70} tend to form crystals that display some degree of disorder and dynamical processes involving various rotations of the fullerene [19–25]. However, in the two co-crystallized materials, $C_{70} \cdot 2\{(\eta^5\text{-}C_5H_5)_2Fe\}$and $C_{70} \cdot 6(S_8)$, the C_{70} molecules assume fully ordered positions and are free of rotational dynamics that complicate structure determinations. Table 2 presents a comparison of bond lengths within C_{70} that are taken from a variety of sources. These include the present structure of $C_{70} \cdot 2\{(\eta^5\text{-}C_5H_5)_2Fe\}$, the single crystal X-ray diffraction study of $C_{70} \cdot 6(S_8)$ [26], a pulsed neutron diffraction study of C_{70} powder at 300 K, an electron diffraction study of a C_{70} film at room temperature [27], and a gas phase electron diffraction study of C_{70} at 825°C [28]. While there is generally good agreement among the parameters obtained from these five studies of unaltered C_{70}, the studies do show variation in the length of the equatorial e–e bond. Thus, this bond is unusually short in the solid state electron diffraction study and considerably elongated in the high temperature, gas phase electron diffraction study. Theoretical calculations on the structure of C_{70} at 825°C do not reproduce the electron diffraction data and do not show any cause for exceptional lengthening of the e–e bond [29].

Table 2
Bond lengths within C_{70}

Bond	$C_{70} \cdot 2\{(\eta^5\text{-}C_5H_5)_2Fe\}$[a]	$C_{70} \cdot 5(S8)$[b]	C_{70} (solid)[c]	C_{70} (solid)[d]	C_{70} (gas phase)[e]
a–a	1.451(13)	1.451(3)	1.464(9)	1.460(4)	1.461(8)
a–b	1.397(12)	1.387(4)	1.37(1)	1.382(6)	1.388(16)
b–c	1.436(16)	1.445(3)	1.47(1)	1.449(5)	1.453(11)
c–c	1.391(16)	1.378(3)	1.37(1)	1.396(6)	1.386(25)
c–d	1.441(12)	1.447(2)	1.46(1)	1.464(7)	1.405(13)
d–d	1.439(14)	1.426(3)	1.47(3)	1.420(4)	1.425(14)
d–e	1.416(10)	1.414(2)	1.39(1)	1.415(5)	1.405(13)
e–e	1.469(10)	1.462(10)	1.41(3)	1.477(6)	1.538(19)

[a] This work, single crystal X-ray diffraction.
[b] From Ref. [22], single crystal X-ray diffraction.
[c] From Ref. [23], powder electron diffraction.
[d] From Ref. [16], powder pulsed neutron diffraction.
[e] From Ref. [24], gas phase electron diffraction.

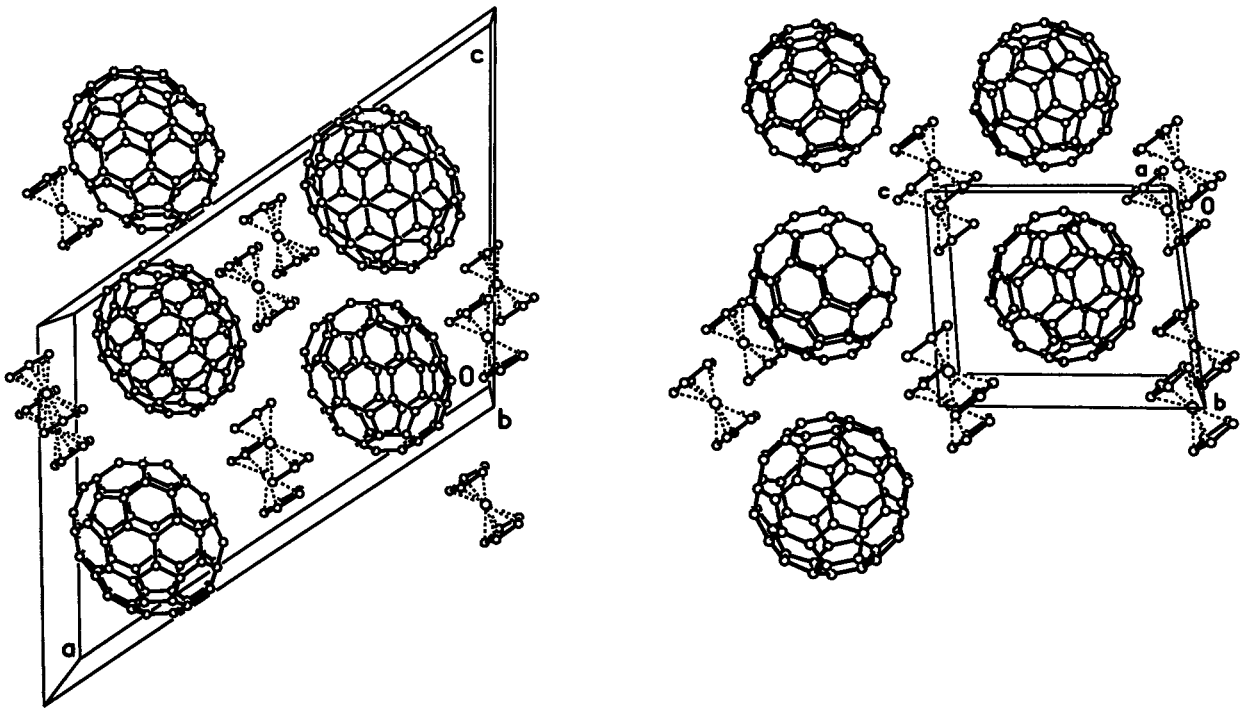

Fig. 5. A comparison of the molecular packing in $C_{70} \cdot 2\{(\eta^5\text{-}C_5H_5)_2Fe\}$ and $C_{60} \cdot 2\{(\eta^5\text{-}C_5H_5)_2Fe\}$. Data for $C_{60} \cdot 2\{(\eta^5\text{-}C_5H_5)_2Fe\}$ were taken from Ref. [22].

4. Experimental

The reactions were performed under a purified atmosphere of dinitrogen with the use of Schlenk techniques unless otherwise noted. The solvents were degassed before use. $Pd(PPh_3)_4$ was synthesized according to a reported procedure [30]. Infrared spectra were recorded on a Galaxy Series FTIR 3000 spectrometer as KBr pellets. NMR spectra were recorded on a QE-300 instrument. $^{31}P\{^1H\}$-NMR spectra were referenced to external 85% H_3PO_4 in H_2O, with downfield chemical shifts reported as positive.

4.1. Preparation of $(\eta^2\text{-}C_{70})Pd(PPh_3)_2$

To a solution of C_{70} (36 mg, 0.043 mmol) in benzene (7 ml), $Pd(PPh_3)_4$ (49 mg, 0.043 mmol) was added. The red–brown solution was stirred for 10 min. The solvent was then removed under vacuum. The brown solid was redissolved in dichloromethane (1 ml), and the solution was filtered. Diethyl ether (40 ml) was added to the filtrate to precipitate the product as a black crystalline solid in 91% yield. IR (KBr pellet): 1431 (vs), 1411 (m), 1092 (m), 742 (s), 692 (vs), 673 (m), 579 (m), 534 (m), 513 (s, br), 457 (m). For comparison, IR spectrum of C_{70} in KBr pellet displayed bands at 1429 (vs), 1414 (s), 1134 (m), 795 (s), 674 (s), 642 (m), 577 (s), 564 (m), 534 (s), 459 (m). NMR (in toluene-d_8): at -80°C, $\delta = 29.2$ [d, 1P, $^2J(P, P) = 8$ Hz], 26.7 [d, 1P, $^2J(P, P) = 8$ Hz]; at 25°C, $\delta = 29.3$ [s, 1P], 26.9 [s, 1P]; at 80°C, $\delta = 27.9$ [s, br, 2P]; at 100°C, $\delta = 28.2$ [s, sharp, 2P].

4.2. Preparation of $C_{70} \cdot 2\{(\eta^5\text{-}C_5H_5)_2Fe\}$

A saturated carbon disulfide solution of C_{70} was mixed with an equal volume of a saturated carbon disulfide solution of ferrocene. The resulting reddish solution was allowed to slowly evaporate without disturbing for two weeks. Shiny black crystals of product,

Table 3
Crystal data and data collection parameters

	$(\eta 2\text{-}C_{70})Pd(PPh_3)_2 \cdot CH_2Cl_2$	$(C_{70}) \cdot 2\{\eta^5\text{-}C_5H_5)_2Fe\}$
Empirical formula	$C_{107}H_{32}Cl_2P_2Pd$	$C_{180}H_{40}Fe_4$
Formula weight	1556.57	2425.52
T (K)	130(2)	130(2)
Color, habit	Black, plate	Black, plate
Crystal system	Monoclinic	Monoclinic
Space group	$P2_1/n$	$C2$
a (Å)	18.309(2)	27.752(5)
b (Å)	14.325(2)	10.056(2)
c (Å)	23.796(2)	19.603(6)
β (°)	92.428(7)	124.19(2)
Z	4	2
ρ (g cm^{-3})	1.658	1.780
μ (mm^{-1})	4.175	5.666
R^a (obsd data)	0.093	0.076
wR_2	0.202	0.201

[a] $R_1 = \Sigma\|F_o - F_c\|/\Sigma|F_o|$; $wR_2 = [\Sigma[\omega(F_o^2 - F_c^2)^2]/\Sigma[\omega(F_o^2)^2]]^{1/2}$.

$C_{70} \cdot 2\{(\eta^5\text{-}C_5H_5)_2Fe\}$, were separated from the orange crystals of ferrocene by hand.

4.3. X-ray data collection for $(\eta^2\text{-}C_{70})Pd(PPh_3)_2 \cdot CH_2Cl_2$ and $C_{70} \cdot 2\{(\eta^5\text{-}C_5H_5)_2Fe\}$

Well-shaped black crystals of $(\eta^2\text{-}C_{70})Pd(PPh_3)_2 \cdot CH_2Cl_2$ were obtained by slow diffusion of diethyl ether into a dichloromethane solution of the complex. Crystals of $C_{70} \cdot 2\{(\eta^5\text{-}C_5H_5)_2Fe\}$ were selected from the mass of crystals prepared as described above. Suitable crystals of these compounds were coated with a light hydrocarbon oil and mounted in the 130 K dinitrogen stream of a Syntex $P2_1$ diffractometer equipped with a locally modified low temperature apparatus. Intensity data were collected using graphite monochromated Cu–Kα radiation (λ 1.54178 Å). Crystal data for both compounds are given in Table 3. Two check reflections showed only random ($< 1\%$) variation in intensity during data collection. The data were corrected for Lorentz and polarization effects.

4.4. Solution and structure refinement

Calculations were performed with SHELXTL 5 series of programs. Scattering factors and correction for anomalous dispersion were taken from a standard source [31]. Absorption corrections were applied [32]. The solutions were determined by direct methods and subsequent cycles of least-squares refinement and calculation of difference Fourier maps. For $(\eta^2\text{-}C_{70})Pd(PPh_3)_2 \cdot CH_2Cl_2$, the data to parameter ratio justified anisotropic refinement for only the heavy atoms, Pd, Cl and P.

5. Supplementary material

Crystallographic data for the structural analysis have been deposited with the Cambridge Crystallographic Data Centre, CCDC No. 1022221 for $(\eta^2\text{-}C_{70})Pd(PPh_3)_2 \cdot CH_2Cl_2$ and CCDC No. 102223 for $C_{70} \cdot 2\{(\eta^5\text{-}C_5H_5)_2Fe\}$. Copies of this information may be obtained free of charge from The Director, CCDC, 12 Union Road, Cambridge, CB2 1EZ, UK (Fax: +44-1223-336-033; e-mail: deposit@ccdc.cam.ac.uk or www:http://www.ccdc.cam.ac.uk).

Acknowledgements

The authors thank the US National Science Foundation (Grant CHE 9610507) for support and Johnson Matthey for a loan of palladium(II) chloride.

References

[1] A.L. Balch, M.M. Olmstead, Chem. Rev. 98 (1998) 2123.
[2] A.H.H. Stephens, M.L.H. Green, Adv. Inorg. Chem. 44 (1997) 1.
[3] A.L. Balch, The chemistry of fullerenes, in: R. Taylor (Ed.), Advanced Series in Fullerenes, vol. 4, World Scientific Publishing, Singapore, 1995, p. 220.
[4] A.L. Balch, V.J. Catalano, J.W. Lee, M.M. Olmstead, S.R. Parkin, J. Am. Chem. Soc. 113 (1991) 8953.
[5] A.L. Balch, J.W. Lee, M.M. Olmstead, Angew. Chem. Int. Ed. Engl. 31 (1992) 1356.
[6] H.-F. Hsu, J.R. Shapley, J. Chem. Soc. Chem. Commun. (1997) 1125.
[7] A.L. Balch, L. Hao, M.M. Olmstead, Angew. Chem. Int. Ed. Engl. 35 (1996) 188.
[8] J.M. Hawkins, A. Meyer, M.A. Solow, J. Am. Chem. Soc. 115 (1993) 7499.
[9] H.-F. Hsu, Y. Du, T.E. Albrecht-Schmitt, S.R. Wilson, J.R. Shapley, Organometallics 17 (1998) 1756.
[10] J.M. Hawkins, A. Meyer, Science 260 (1993) 1918.
[11] J.M. Hawkins, M. Nambu, A. Meyer, J. Am. Chem. Soc. 116 (1994) 7642.
[12] A.L. Balch, A.S. Ginwalla, B.C. Noll, M.M. Olmstead, J. Am. Chem. Soc. 116 (1994) 2227.
[13] R.C. Haddon, Science 261 (1993) 1545.
[14] V.V. Bashilov, P.V. Petrovskii, V.I. Sokolov, S.V. Lindeman, I.A. Guzey, Y.T. Struchkov, Organometallics 12 (1993) 991.
[15] J.D. Crane, P.B. Hitchcock, H.W. Kroto, R. Taylor, D.R.M. Walton, J. Chem. Soc. Chem. Commun. (1992) 1764.
[16] J.D. Dunitz, L.E. Orgel, A. Rich, Acta Crystallogr. 9 (1956) 373.
[17] R.K. Bohn, A. Haaland, J. Organometal. Chem. 5 (1966) 470.
[18] G.J. Palenik, Inorg. Chem. 9 (1970) 2424.
[19] J. Janaki, G.V.N. Rao, V.S. Sastry, Y. Hariharan, T.S. Radhakrishnan, C.S. Sundar, A. Bharati, M.C. Valsakumar, N. Subramanian, Solid State Commun. 94 (1995) 37.
[20] A.V. Nikolaev, T.J.S. Dennis, K. Prassides, A.K. Soper, Chem. Phys. Lett. 223 (1994) 143.
[21] C. Christides, T.J.S. Dennis, K. Prassides, R.L. Cappelletti, D.A. Neumann, J.R.D. Copley, Phys. Rev. B 49 (1994) 2897.
[22] C. Meingast, F. Gugenberger, G. Roth, M. Haluska, H. Kuzmany, Z. Phys. B 95 (1994) 67.
[23] E. Blanc, H.-B. Bürgi, R. Restori, D. Schwarzenbach, P. Stellberg, P. Venugopalan, Europhys. Lett. 27 (1994) 359.
[24] T. Mitsuki, Y. Ono, H. Horiuchi, J. Li, N. Kino, K. Kishio, K. Kitazawa, Jpn. J. Appl. Phys. 33 (1994) 6281.
[25] D.L. Dorset, J.R. Fryer, J. Phys. Chem. 111 (1997) 3968.
[26] H.B. Bürgi, P. Venogopalan, D. Schwarzenbach, F. Diederich, C. Thilgen, Helv. Chim. Acta 76 (1993) 2155.
[27] D.R. McKenzie, C.A. Davis, D.J.H. Cockayne, D.A. Muller, A.M. Vassallo, Nature 355 (1992) 622.
[28] K. Hedberg, L. Hedberg, M. Buhl, D.S. Bethune, C.A. Brown, R.D. Johnson, J. Am. Chem. Soc. 119 (1997) 5314.
[29] T.Z. Mordasini, C. Hanser, W. Thiel, Chem. Phys. Lett. 288 (1998) 183.
[30] D.R. Coulson, Inorg. Synth. 28 (1990) 107.
[31] A.J.C. Wilson (Ed.), *International Tables for Crystallography*, Volume C, Kluwer Academic Publishers, Dordrecht, 1992.
[32] S. Parkin, B. Moezzi, H. Hope, J. Appl. Crystallogr. 28 (1995) 53.